IOP Conference Series: Earth and Environmental Science

PAPER • OPEN ACCESS

# Analysis of operating modes of electric drives in agriculture

To cite this article: A T Tsirkunenko and Y S Zagoskin 2019 *IOP Conf. Ser.: Earth Environ. Sci.* **315** 032041

# Analysis of operating modes of electric drives in agriculture

**A T Tsirkunenko[1] and Y S Zagoskin[2]**

[1] RiK-Energo lld, Ekaterinburg, Russian Federation
[2] Emerson, Russian Federation

E-mail: m9191236713@mail.ru

**Abstract**. An algorithm for analyzing the operating modes of an agriculture electric machine as a control object based on its generalized mathematical model using the Fourier transform of non-sinusoidal signals of phase currents and conductance along the air gap of an electric machine is proposed, which is applicable to any electric machine with magnetic non-symmetry of rotor and which allows to obtain and investigate the spectral composition of such electric drive's coordinates as induction and electromagnetic torque. According to such an algorithm, it is recommended to perform the calculation under the following assumptions: the machine is not saturated, the magnetic conductivity of steel is equal to infinity, there are no scattering fluxes. When going beyond these limitations, the calculation must be refined by a numerical finite element method using Maxwell's equations. An example of an agriculture electric drive with a synchronous reluctance machine of independent excitation coordinates calculations is given according to the proposed algorithm in comparison with a numerical calculation by the finite element method.

## 1. Introduction
Due to significant progress in the field of power and information electronics, the development of agriculture electric machines' active materials, nowadays electromechanics and electric drive are developing in the direction of research and improvement of non-traditional electric machines and electric drives based on them. Examples are synchronous reluctance and inductor agriculture AC drives [1]. Distinctive features: the electromagnetic torque is created only by the magnetic non-symmetry of the rotor; the number of phases, the shape of the phase currents and voltages are arbitrary [2]. Advantages of non-traditional electric machines and agriculture electric drives based on them are: the ability to work in an extended range of speeds, work with large overloads up to 4 times and higher, high specific weight and size indicators, manufacturability [3]. That is why the task of improving the consumer properties of such electromechanical complexes due to optimization of operating modes is actual [4].

## 2. Formulation of the research problem
The aim of the study is to obtain a calculation algorithm for analyzing the operating modes of any electric machine of a non-traditional design with magnetic non-symmetry of rotor operating within the regulated agriculture electric drive from the position of synthesis of the control system, i.e. obtaining the relationship between the laws of control and the electromagnetic torque, the speed with the possibility of spectral analysis of these variables.

To achieve this goal, it is necessary to solve the following tasks:

- development of the method for spectral analysis of variables;
- development of an algorithm for analyzing the operating modes of the control object;
- checking the adequacy of the developed methods and algorithms.

## 3. The idea of spectral analysis of distributions of variables

The expansion of the slot currents' density distribution function I (x, t) along the stator boring in the interval [0; 2π] in a Fourier series will be carried out according to the known formulas (1) [5].

The I (x, t) distribution function of the slot currents can be represented as a set of constant currents relative to x located at certain intervals, where the Fourier coefficients [6] can be calculated as follows (2).

$$I(x,t,\alpha) = \frac{a_0(t)}{2} + \sum_{k=1}^{\infty}\left(a_k(t)\cdot\cos(k\cdot[x+\alpha]) + b_k(t)\cdot\sin(k\cdot[x+\alpha])\right)$$
$$S(x,t,\alpha) = \frac{a_0(t)}{2} + \sum_{k=1}^{n}\left(a_k(t)\cdot\cos(k\cdot[x+\alpha]) + b_k(t)\cdot\sin(k\cdot[x+\alpha])\right)$$
$$\Delta = \frac{1}{\pi}\cdot\int_0^{2\cdot\pi}\left(I(x,t,\alpha) - S(x,t,\alpha)\right)^2 dx$$
$$a_0(t) = \frac{1}{\pi}\cdot\int_0^{2\cdot\pi} I(x,t)\,dx \tag{1}$$
$$a_k(t) = \frac{1}{\pi}\cdot\int_0^{2\cdot\pi} I(x,t)\cdot\cos(k\cdot x)\,dx$$
$$b_k(t) = \frac{1}{\pi}\cdot\int_0^{2\cdot\pi} I(x,t)\cdot\sin(k\cdot x)\,dx$$
$$A_k = \sqrt{a_k(t)^2 + b_k(t)^2}$$
$$\varphi_k = \operatorname{arctg}(\frac{b_k(t)}{a_k(t)})$$

$$a_0(t) = \frac{2}{\pi}\cdot\sum_{j=0}^{m-1} I_j(t)\cdot\frac{\pi}{m}$$
$$a_k(t) = \frac{1}{\pi}\cdot\sum_{j=0}^{m-1}\frac{I_j(t)}{k}\cdot\left(\sin\left(k\cdot 2\cdot\pi\cdot\frac{j+1}{m}\right) - \sin\left(k\cdot 2\cdot\pi\cdot\frac{j}{m}\right)\right) \tag{2}$$
$$b_k(t) = \frac{1}{\pi}\cdot\sum_{j=0}^{m-1}\frac{I_j(t)}{k}\cdot\left(\cos\left(k\cdot 2\cdot\pi\cdot\frac{j+1}{m}\right) - \cos\left(k\cdot 2\cdot\pi\cdot\frac{j}{m}\right)\right)$$

where *I*j is the magnitude of the slot current; m is the number of intervals for partitioning the common range [0; 2π].

After transforming the substraction of trigonometric functions into a product, we get:

$$a_0(t) = \frac{2}{\pi}\cdot\sum_{j=0}^{m-1} I_j(t)$$
$$a_k(t) = \frac{2}{\pi\cdot k}\cdot\sin(\frac{k\cdot\pi}{m})\cdot\sum_{j=0}^{m-1} I_j(t)\cdot\cos(k\cdot 2\cdot\pi\cdot\left[\frac{2\cdot j+1}{2\cdot m}\right]) \tag{3}$$
$$b_k(t) = \frac{2}{\pi\cdot k}\cdot\sin(\frac{k\cdot\pi}{m})\cdot\sum_{j=0}^{m-1} I_j(t)\cdot\sin(k\cdot 2\cdot\pi\cdot\left[\frac{2\cdot j+1}{2\cdot m}\right])$$

The Fourier expansion method allows to obtain algorithms for calculating the generalized mathematical model [7]. This method is convenient because the operations of integration and differentiation are easily realizable due to the representation of variables in the form of the indicated series [8].

## 4. Algorithm for analyzing the operating modes of the control object

The algorithm for analyzing the operating modes (figure 1) is based on the generalized mathematical model of the electric machine presented in [9, 10].

At the stage number 1, it is necessary to determine the number *m* of equal intervals of the air gap length splitting [11]. The larger the number of intervals, the more accurate it is possible to construct the distribution functions of coordinates along the air gap [12].

At the stage number 2, the distribution of the slot currents is represented as a vector that changes as a function of time:

$$\overrightarrow{Ip(t)} = (f_1(t) \dots f_m(t)) \quad (4)$$

At the stage number 3, the distribution of the slot currents is decomposed into a Fourier series for convenience of further analysis by the method described above [13, 14].

At the stage number 4, the MDS distribution is obtained by integrating the distribution of the slot currents as a Fourier series along the coordinate *x* along the air gap:

$$f(x,t) = \int I(x,t)dx \quad (5)$$

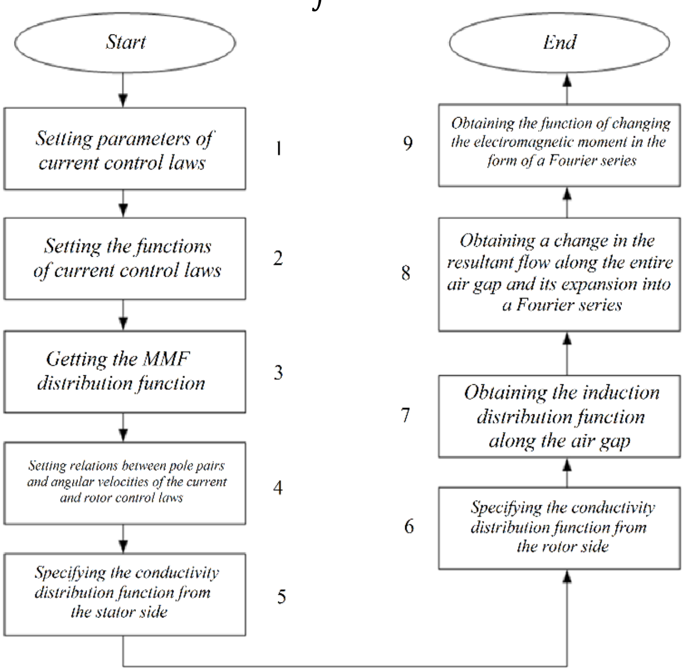


**Figure 1.** Algorithm for analysis of the electric machine.

At the stage number 5, the distribution of conductances from the stator side is given in the form of a vector consisting of constant values of conductivity with subsequent Fourier expansion and obtaining the function *Zst* (*x*):

$$\overrightarrow{Zst} = (Cst_1 \dots Cst_m) \quad (6)$$

At the stage number 6, the distribution on the rotor side is also set in the form of a vector consisting of constant values of conductivity with subsequent Fourier expansion [15] and obtaining the function *Zrot* (*x*, *α*), where α is the angle of rotation of the rotor:

$$\overrightarrow{Zrot} = (Crot_1 \dots Crot_m) \quad (7)$$

At the stage number 7 we obtain the induction distribution along the air gap [16]:

$$F(x,t,\alpha) = f(x,t) \cdot Zst(x) \cdot Zrot(x,\alpha) \quad (8)$$

At the stage number 8, we integrate the module of the function (8) along the entire length of the air gap [17]:

$$Fsum(t,\alpha) = \int_{0}^{2\pi} |F(x,t,\alpha)| dx \quad (9)$$

At the stage number 9, we differentiate the function (9) along the rotation angle of the rotor to obtain a value proportional to the electromagnetic torque of the electric machine [18]:

$$M(t,\alpha) = \frac{\partial Fsum(t,\alpha)}{\partial \alpha} \quad (10)$$

## 5. Results of algorithm application

For an example, we calculate the induction distributions along the air gap and the electromagnetic torque as a function of the rotor angle of the synchronous independent excitation reluctance machine (SIERM) [19], which operates as part of a regulated agriculture electric drive. The calculation is comparable with the similar analysis by the finite element method [20, 21]. Conditions for obtaining output coordinates: induction is calculated for one instant of time, when the electromagnetic torque is maximum; the torque is calculated for half the electric rotor revolution [22, 23].

**Table 1.** Parameters and nominal values of the electrical machine.

| Parameter name | Value |
|---|---|
| Rated power $P_N$, kW | 16 |
| Nominal speed $\omega_H$, rad/s | 157 |
| Rated torque $M_N$, N·m | 100 |
| External dimension of the stator core $D_a$, mm | 254 |
| Internal diameter of the stator $D$, mm | 158 |
| The magnitude of the pole arc from pole division, $\alpha_p$ | 0,5 |
| Length of the stator core $l_\delta$, mm | 184 |
| Number of stator teeth $Z_1$ | 48 |
| Number of phases $m$ | 6 |
| Number of poles $2p$ | 4 |
| Nominal phase voltage $U_N$, V | 75 |
| Nominal current $I_N$, A | 50 |
| Linear load, A/cm | 410 |
| The calculated value of the induction $B_\delta$, T | 1 |
| Single-sided air gap $\delta$, mm | 1 |
| Diameter of the rotor, mm | 156 |

The distribution of the slot currents has the form:

$$\boldsymbol{Ip} = (0\ 1\ 0\ 1\ 0\ 1\ 0\ 1\ 0\ 1\ 0\ 1\ 0\ 1\ 0\ 1\ 0\ 1\ 0\ 1\ 0\ 1\ 0\ 1\ 0\ {-1}\ 0\ {-1}\ 0\ {-1}\ 0\ {-1}\ 0\ {-1}\ 0\ {-1}\ 0\ {-1}\ 0\ {-1}\ 0\ {-1}\ 0\ {-1}\ 0\ {-1}\ 0\ {-1}) \quad (11)$$

The distribution of stator conductances is:

IOP Conf. Series: Earth and Environmental Science **315** (2019) 032041 doi:10.1088/1755-1315/315/3/032041

***Zst*** = (1 0.4 1 0.4 1 0.4 1 0.4 1 0.4 1 0.4 1 0.4 1 0.4 1 0.4 1 0.4 1 0.4 1 0.4 1 0.4 1 0.4 1 0.4 1 0.4 1 0.4 1 0.4 1 0.4 1 0.4 1 0.4 1 0.4 1 0.4 1 0.4) (12)

The distribution of the rotor conductivity has the form:

***Zrot*** = (1 1 1 1 1 1 1 1 1 1 1 1 1 0.1 0.1 0.1 0.1 0.1 0.1 0.1 0.1 0.1 0.1 0.1 0.1 1 1 1 1 1 1 1 1 1 1 1 10.1 0.1 0.1 0.1 0.1 0.1 0.1 0.1 0.1 0.1 0.1 0.1 1 1 1 1 1 1 1 1 1 1 1 1 1) (13)

In figure 2 the results of calculations based on the proposed mathematical model (curves 1) and the finite element model (curves 2) are shown [24].

A comparison of the induction values along the air gap above the pole division of the SIERM was carried out for two states of the magnetic system: not saturated (figure 2a) and at the saturation boundary (figure 2b) [25]. The calculation time torque corresponds to the current maximum value of the electromagnetic torque. The accuracy of the synthesized mathematical model in the absence of saturation is higher than the accuracy with a saturated state of the magnetic system [26]. This is due to the redistribution of conductivity when the magnetic system is saturated, because the magnetization curve is not linear [27]. As a consequence, an increase in the lower values of induction occurs (Figure 2b, curve 2), i.e. flattening of the induction curve [28, 29]. The inaccuracy of the induction teeth width is explained by the complicated shape of the slot, which is not taken into account in the proposed model. The error in the difference between the maximum and minimum induction values can be reduced while adjusting the analytical model by specifying the desired difference in the maximum and minimum values of the stator conductivity after the finite element calculation [30, 31].

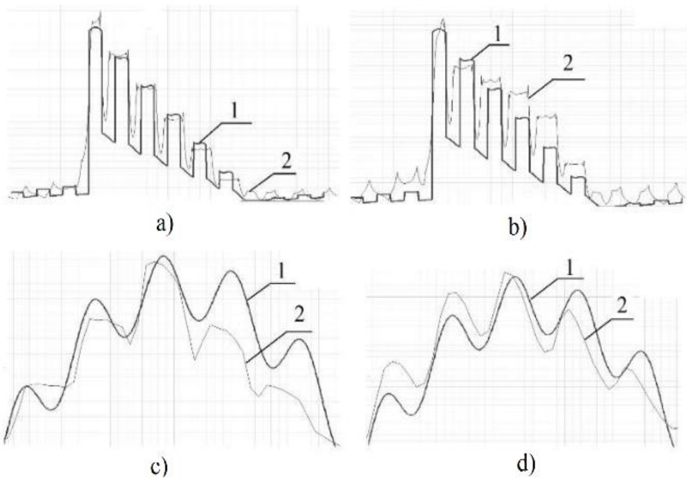

**Figure 2.** Results of calculations and their comparison.

A comparison of the electromagnetic torque values was also carried out for two states of the magnetic system: not saturated (figure 2c) and saturated (figure 2d). For both states, the error is due to the integral error in calculating the induction along the air gap [32]. The "toothed" nature of the torque curve is explained by the uneven change in the energy of the magnetic field when the rotor is displaced due to the presence of teeth on the stator [33]. At the position of the edges of the poles over the slots and the passage of the entire width of the slot, the integral value of the magnetic flux along the entire air gap practically does not change, this leads to a sharp decrease in the angular torque [34]. In the case of finding the edges of the poles above the stator teeth during its rotation, the magnetic flux along the entire air gap changes significantly and the electromagnetic torque increases [35, 36].

## 6. Practical results

The proposed method can be successfully used in calculations of thermal losses in the magnetic circuit of an electrical machine with non-sinusoidal feeding at the stages of designing an agriculture electric drive. In [37, 38] the results of classical methods and the proposed algorithm are compared. Analysis of the results showed that the accuracy of the calculations is significantly increased by 10-15% [39].

## 7. Conclusion

According to the results of the study, the following conclusions can be drawn:

1. A method for spectral analysis of variables is developed, which is based on the principle of partitioning the distribution functions of variables into intervals where they are constant. This allows to do simple integration and differentiation of the agriculture electric drive's coordinates, represented in the form of a Fourier series in an analytical way;
2. A calculation algorithm for analyzing the operating modes of any electric machine as a control object is developed, based on the method of spectral analysis of variables using a generalized mathematical model that combines the energy approach to electromechanical transformation and the method of winding functions;
3. An example is given of using the algorithm for analyzing the operating modes of an agriculture electric drive to obtain the distribution of induction and force as a function of the rotational angle of a synchronous independent excitation reaction machine, confirming its adequacy. The results are qualitatively close to a similar calculation by the finite elements method.

## References

[1] Grigor'ev M A 2017 *Russian Electrical Eng.* **88**(4) 189-92
[2] Kachesova L Y and Nikol'skii O K 2018 *Russian Electrical Eng*. **89**(12) 681-4
[3] Nesterin V A, Genin V S, Romanov R A and Tokmakov D A 2017 *Russian Electrical Eng*. **88**(7) 400-3
[4] Titov E V, Soshnikov A A, and Drobyazko O N 2018 *Russian Electrical Eng*. **89**(12) 714-6
[5] Nemtsov M V and Trifanov G D 2017 *Russian Electrical Eng*. **88**(5) 285-8
[6] Khizhnyakov Y N, Yuzhakov A A and Titov Y K 2017 *Russian Electrical Eng*. **88**(11) 621-6
[7] Chupin S A and Grigor'ev M A 2018 *Russian Electrical Eng.* **89**(4) 240-4
[8] Sudakov A I and Kamenskikh I A 2018 *Russian Electrical Eng.* **89**(11) 652-7
[9] Zhuravlev A M and Grigor'ev M A 2018 *Russian Electrical Eng.* **89**(4) 222-7
[10] Kolpakhchyan P G, Shcherbakov V G, Kochin A E and Shaikhiev A R 2017 *Russian Electrical Eng*. **88**(5) 259-64
[11] Kavalerov B V, Kilin G A, Chabanov E A, Bakhirev I V and Zhdanovskii E O 2017 *Russian Electrical Eng*. **88**(11) 675-8
[12] Kulikova L V, Evmenchik A S and Delyagin V N 2018 *Russian Electrical Eng*. **89**(12) 689-94
[13] Antipov V N, Grozov A D and Ivanova A V 2017 *Russian Electrical Eng*. **88**(2) 55-60
[14] Gryzlov A A, Grigor'ev M A and Imanova A A 2017 *Russian Electrical Eng.* **88**(4) 193-6
[15] Bakhvalov Y A, Gorbatenko N I, Grechikhin V V and Yufanova A L 2017 *Russian Electrical Eng*. **88**(1) 15-8
[16] Khizhnyakov Y N, Yuzhakov A A, Besukladnikov I I and Trushnikov D N 2018 *Russian Electrical Eng*. **89**(11) 648-51
[17] Kulinich Y M and Shukharev S A 2016 *Russian Electrical Eng*. **87**(9) 532-5
[18] Shcherbinin A G, Subbotin E V and Savchenko V G 2018 *Russian Electrical Eng*. **89**(11) 617-20
[19] Belykh I A, Grigor'ev M A and Belousov E V 2017 *Russian Electrical Eng.* **88**(4) 205-8
[20] Savrasov F V 2017 *Russian Electrical Eng*. **87**(7) 421-4
[21] Petrochenkov A B 2018 *Russian Electrical Eng*. **89**(11) 627-62
[22] Nikol'skii OK, Shlionskaya Y D, Shanygin I A 2018 *Russian Electrical Eng*. **89**(12) 707-13
[23] Mamaev V A, Kononova N N and Murav'ev K A 2016 *Russian Electrical Eng*. **87**(7) 373-7
[24] Gryzlov A A and Grigor'ev M A 2018 *Russian Electrical Eng.* **89**(4) 245-8
[25] Faizrakhmanov R A, Murzakaev R T, Artem'ev V V, Bakunov R R and Khabibulin A F 2018 *Russian Electrical Eng.* **89**(11) 658-63
[26] Fertikov M G, Dyatlov I Y and Trufanova N M 2018 *Russian Electrical Eng.* **89**(11) 633-6
[27] Drobyazko O N 2018 *Russian Electrical Eng*. **89**(12) 728-32
[28] Khalina T M, Stal'naya M I and Eremochkin S Y 2018 *Russian Electrical Eng*. **89**(12) 717-21

[29] Aleksandrov A V, Kiselev I P and Makarova E I 2016 *Russian Electrical Eng*. **87**(5) 256-29
[30] Belykh I A and Grigor'ev M A 2018 *Russian Electrical Eng.* **89**(4) 234-9
[31] Gorozhankin A N, Gryzlov A A and Khayatov E S 2017 *Russian Electrical Eng.* **88**(4) 201-4
[32] Men'shenin A S and Grigor'ev M A 2018 *Russian Electrical Eng.* **89**(4) 228-33
[33] Pavlenko A V, Gummel' A A, Batishchev D V and Baumbach E 2016 *Russian Electrical Eng*. **87**(4) 189-93
[34] Nosov G V and Trofimovich K A 2016 *Russian Electrical Eng*. **87**(3) 166-71
[35] Belousov E V, Grigor'ev M A and Gryzlov A A 2017 *Russian Electrical Eng.* **88**(4) 185-8
[36] Khayatov E S and Grigor'ev M A 2017 *Russian Electrical Eng.* **88**(4) 197-200
[37] Bagaev A A 2018 *Russian Electrical Eng*. **89**(12) 703-6
[38] Tarasov V A, Petrochenkov A B and Kavalerov B V 2018 Systems *Russian Electrical Eng*. **89**(11) 664-9
[39] Timashev E O, Chirkov D A and Korotaev A D 2018 *Russian Electrical Eng*. **89**(11) 643-7